Journal of Neonatal Surgery
ISSN(Online): 2226-0439
Vol. 14, Issue 3 (2025)
https://www.jneonatalsurg.com

OPEN ACCESS

Nano-Optimization: A Box-Behnken Design Approach and Characterization for Roflumilast-Loaded Silver Nanoparticles

Remya Ravindran[*1], Palayyan Muralidharan[2], Arulkumaran Govindarajan[3]

[*1,2]Chettinad School of Pharmaceutical Sciences, Chettinad Hospital and Research Institute, Chettinad Academy of Research and Education, Kelambakkam,Tamilnadu, India.

[3]KTN College of Pharmacy, Chalavara, Palakkad, Kerala, India.

***Corresponding Author:**

Email ID: remsravindran@gmail.com

Cite this paper as: Remya Ravindran, Palayyan Muralidharan, Arulkumaran Govindarajan, (2025) Nano-Optimization: A Box-Behnken Design Approach and Characterization for Roflumilast-Loaded Silver Nanoparticles. *Journal of Neonatal Surgery*, 14 (3), 212-224.

ABSTRACT

Background: Silver nanoparticles with inimitable physical, chemical, and biological characteristics have high antimicrobial capacity. Roflumilast, a PDE4 inhibitor, has now been investigated for anti-psoriatic efficacy as it reduces hyperproliferation and oxidative stress while improving the skin barrier. This study aimed to design Roflumilast-loaded silver nanoparticles (R-AgNPs) using Box Behnken Design (BBD) for optimization.

Materials and Methods: Silver nanoparticles (AgNPs) were formulated by chemical reduction, Optimized using PVP, Sodium borohydride and silver nitrate concentration. Particle size, Polydispersity index (PDI), Zeta potential(ZP), UV, FTIR, TEM, SEM, Drug release and kinetics studies were performed.

Results: Particle size found to be between 20.64 ±0.91 nm and 176.51±0.24 nm, PDI (0.283 ± 0.87 and 0.608 ± 0.06), and zetapotential (-13.0±0.89mV to – 10.5± 0.02mV). Drug release depicts a burst release pattern, succeeded by sustained release. Characterization studies also gave favourable results.

Conclusion: Optimized R-AgNPs showed improved stability, bioavailability and controlled release. Henceforth nanoparticle delivery systems should be further refined to optimize therapeutic efficacy.

Keywords: *Box Behnken Design, Roflumilast, Silver nanoparticles.*

1. INTRODUCTION

AgNPs have emerged promising in pharmaceutical applications due to potent antimicrobial properties and excellent biocompatibility [1]. Their incorporation with drug enhances therapeutic capability of conventional treatment while providing additional benefits, like mitigating the risk of infections in inflammatory skin disorders [2].

Chronic dermal inflammatory diseases pose a major challenge in terms of their treatment and management [3]. This fact necessitates a focused therapeutic approach that targets inflammation and infection together. Though inflammatory conditions could be very well tackled by Roflumilast, its limited topical bioavailability and possible adverse effects keep it at bay [4].

The study is designed to develop and optimize R-AgNP formulation, incorporating the anti-inflammatory properties of Roflumilast and silver nanoparticles' antimicrobial activity. The formulation is optimized by BBD [5]. This enables minimizing experimental runs, providing analysis of formulation variables that include concentrations of polyvinylpyrrolidone (PVP), sodium borohydride and silver chloride [6]. The design is expected to elevate Roflumilast's bioavailability, thereby increasing therapeutic efficacy and combining protection against microbial infections. This allows better patient responses ultimately decreasing complications that arise from chronic dermal inflammatory conditions.

2. MATERIALS AND METHODS

Materials:

Roflumilast was received from Combi-Blocks, USA. Polyvinyl Pyrrolidone (PVP), Sodium Borohydride, Trisodium Citrate, and Silver Nitrate from Chemind Chemicals, Kerala, India

Methods

Design of experiment - The Optimization:

Analysis of effect of three independent variables at multiple levels on dependent variables was done by BBD [7]. Independent variables considered were concentrations of PVP, Sodium Borohydride, and Silver Nitrate, taken as Factors 1, 2 and 3 respectively and three levels identified for each[8]. Particle size, PDI, and zeta potential are the responses as in table I&II [9].

Table I: Different levels of independent factors

Independent factors	High level	Mid-level	Low level
Concentration of PVP (mg)	150	100	50
Concentration of Sodium Borohydride(mg)	60	40	20
Concentration of Silver Nitrate(mg)	150	100	50

Table II: Factors and responses.

	Factor 1	Factor 2	Factor 3	Response 1	Response 2	Response 3
Run	**A:PVP**	**B:sodium borohydrate**	**C:silver nitrate**	**particle size**	**PDI**	**zeta potential**
	mg	Mg	mg	nm		mV
1	100	20	150	86.3	0.393	-13
2	150	40	150	61.35	0.498	-23.4
3	100	40	100	21.64	0.641	-21.5
4	50	40	150	57.42	0.514	-11.78
5	150	20	100	150	0.432	-15.73
6	100	40	100	23.25	0.608	-20.1
7	100	60	150	74.47	0.531	-20.94
8	50	60	100	71.3	0.653	-19.3
9	150	60	100	110.75	0.521	-16.5
10	100	20	50	130	0.283	-12
11	100	60	50	98.44	0.64	-10.5
12	50	40	50	60.87	0.41	-11.1
13	100	40	100	20.64	0.531	-20.5
14	100	40	100	21.44	0.511	-19.1
15	150	40	50	176.51	0.552	-15.25
16	100	40	100	31.64	0.431	-18.5
17	50	20	100	73.67	0.5	-11.57

Design comprised 17 experimental runs, including 12 factorial design runs and 5 centre points [10] and matrix developed using Design Expert 13.0 (State Ease) software [11]. Model statistics and ANOVA analysis were carried out.

Preparation of R-AgNPs:

Chemical reduction was applied in synthesis of silver nanoparticles [12]. Nanoparticle synthesis solution of silver nitrate and PVP was done in distilled water (50 mL). Sodium borohydride solution introduced dropwise to the mixture over a period of 10-minutes under continuous stirring at 1000 RPM. Resulting particles were separated via centrifugation and washed with distilled water for multiple times. Nanoparticles were then combined with 1mg/ml Roflumilast solution, sonicated at 40KHz for 30 minutes, and incubated at room temperature for 24 hours. Finally, drug-loaded particles were centrifuged and washed thoroughly in distilled water [13].

Characterization:

Particle size, PDI and ZP determination:

Measurement of Particle size, PDI and Zeta potential were done using dynamic light scattering (DLS) with Malvern Zeta Sizer ZS90 at 90º scattering angle at 25^0C [14].R-AgNPs were sonicated for 5 minutes and diluted in acetonitrile (1:10) before analysis. The zeta potential was inferred using electrophoretic mobility in capillary cell[15]. The reliability of the results was investigated in triplicate.

Encapsulation Efficiency (EE):

EE of R-AgNPs was determined by centrifuging 1ml solution for 30 minutes, at 15,000 rpm, to separate Roflumilast from nanoparticles. The supernatant was collected, filtered through 0.25µm filter and absorbance was taken using UV-visible spectrophotometry at 251 nm to determine concentration of the free drug [16]. EE was analysed by identifying the difference between initial drug amount and quantity present in supernatant [17]. Calculation of Encapsulation efficiency was done using:

$$EE\ (\%) = \frac{\text{Amount of drug present in nanoparticle}}{\text{Total amount of drug added}} \times 100$$

Fourier Transform Infrared Spectroscopy (FT-IR) Analysis:

KBR pellet method is employed in FTIR analysis wherein the drug and excipient analysis and compatibility studies were undergone [18]. In a hydraulic press, the samples were compressed to form discs. Shimadzu FTIR 8400 S instrument was used for maximum possible detection, with the opted wavelength range between 400cm^{-1} and 4000cm^{-1}.

Surface morphology characterization:

Scanning Electron Microscopy (SEM):

The surface morphology of R-AgNPs were interpreted employing SEM at a magnification of 40,000X and an accelerating voltage of 5.00 Kv [19]. At this magnification range, the imaging provides topographical attributes assessing the reliability as a formulation. A 5µl dispersion of nanoparticles was introduced to carbon coated copper grid, 6 hours of vacuum was applied at room temperature to dry the grid to eliminate moisture. After drying, grid was kept on the SEM sample holder and observed under electron beam.

Transmission electron microscopy (TEM):

Three-dimensional structure of R-AgNPs was retrieved by Jeol/JEM 2100 microscope at voltage of 200 kV [20]. Fitted with a LaB_6 electron gun, it delivers a highly resolved image at point resolution of 0.23 nm and a lattice resolution of 0.14 nm. Nanoparticle dispersion was introduced on a copper grid containing a carbon film, and air-dried to remove leftover solvent and analysis was performed at 120 kV.

***In vitro* release analysis:**

Modified Franz diffusion cell was applied to assess *in vitro* release of Roflumilast from silver nanoparticles [21].Cellulose acetate membrane (molecular threshold – 10 to 12 KDa) separates the donor and receptor compartments, with the latter(12 ml capacity) filled with phosphate-buffered saline (PBS, pH 7.4) to mimic physiological conditions. The donor compartment contained the formulation, kept at 37°C±0.5^0c with continuous stirring at 100 rpm. Aliquots were taken at specified intervals (0.5, 1, 2, 4, 8, 12, and 24 hours), from the receptor compartment and replenished with new PBS to maintain sink conditions. Concentration of released drug was analysed via UV-Visible spectroscopy at 247nm. The cumulative % of drug release was interpreted using:

$$\text{Cumulative Release (\%)} = \frac{\text{Amount of drug released at time t}}{\text{Total amount of drug loaded}} \times 100$$

The *in vitro* study data was examined using kinetic modelling to explore the dynamics and mechanism of drug release.

Statistical Data Analysis:

Data analysis for statistical purposes was done using GraphPad Prism software version 10 [20] in triplicate with mean±standard deviation for independent experiments. The findings were confirmed at a threshold of $p<0.005$ by 'one-way ANOVA' and 'one sample student's *t*-test'.

3. RESULTS

Optimisation of Roflumilast loaded silver nanoparticles:

Stat-Ease Design-Expert® software version 13.0 utilized RSM with a three level (low, middle and high), three factorial BBD, to investigate influence of PVP(A), sodium borohydride(B), and silver nitrate(C) on particle size, PDI, and zeta potential. Table 1 shows the range and levels in the study. To streamline process parameters,17 runs were undertaken according to design matrix. AgNPs were prepared by chemical reduction and Roflumilast was loaded successfully and measured for responses. Model statistics for the responses are shown in table III.

Table: III: Model statistics for the responses

Response	R^2	Adjusted R^2	Predicted R^2	Adequate precision
Particle Size	0.9883	0.9732	0.8464	24.909
PDI	0.9421	0.9389	0.8212	10.4723
Zeta potential	0.9982	0.9803	0.8974	14.6294

Determination of particle size:

As shown in table,among 17 runs, the smallest (20.64 nm) was recorded in run 13, while the largest (176.51 nm) in run 15. The polynomial equation for particle size is as follows:

Particle Size = Y0 + 67.069 (Factor 2) - 81.66 (Factor 3) - 72.09 (Factor 2 × Factor 3)

The absence of Factor 1 indicates its minimal effect. Sodium borohydride positively ($p<0.05$) influences particle size, whereas silver nitrate influences negatively($p<0.05$) and their interaction produces a negative impact.

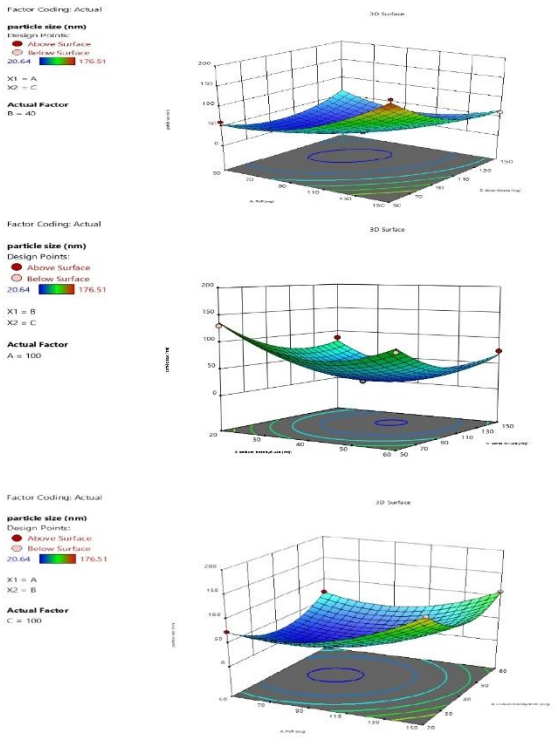

Figure I: Response surface plot (3D) of particle size

Fig I, Owing to high statistical significance, remarkable adjusted (0.9732), predicted R^2 (0.8464) values and acceptable lack of fit value(p=0.0702), Quadratic model was recommended and confirmed by ANOVA (F=65.57, P<0.0001). Significant factors included A, B, C, AB, AC, A^2, B^2, and C^2 ($p < 0.05$). The model revealed model fit with R^2(0.9883), adjusted R^2(0.9732) and predicted R^2(0.8464), having difference <0.2. Adequate precision was 24.91, affirming robustness. B^2 had the highest influence, succeeded by A^2(34.72) and AC (-27.93).

PDI:

The lowest PDI was in run 10(0.283), while the highest PDI in run 6(0.608)The polynomial equation for PDI is as follows:

PDI = 0.3+0.02(Factor 1) +0.01(factor 2)-0.03(factor 3) +0.005(factor2xfactor3)

The concentrations of PVP and sodium borohydride increased PDI, while silver nitrate reduced it, contributing improved particle uniformity. The linear model (sequential p=0.0473, lack of fit p=0.5719, adjusted R2=0.3176, predicted R2=0.0506) was chosen. Amid factors, B was significant (0.0069), whereas A and C were not(p>0.1). Excellent model fit was validated as lack of fit was not significant (F=0.94, p=0.5719).

Adjusted R^2(0.3176) and low predicted R^2(0.0506) recommend limitations, perhaps caused by block effects. The adequate precision ratio (5.146), beyond threshold 4, validates adequate signal to noise ratio, causing model fitting.

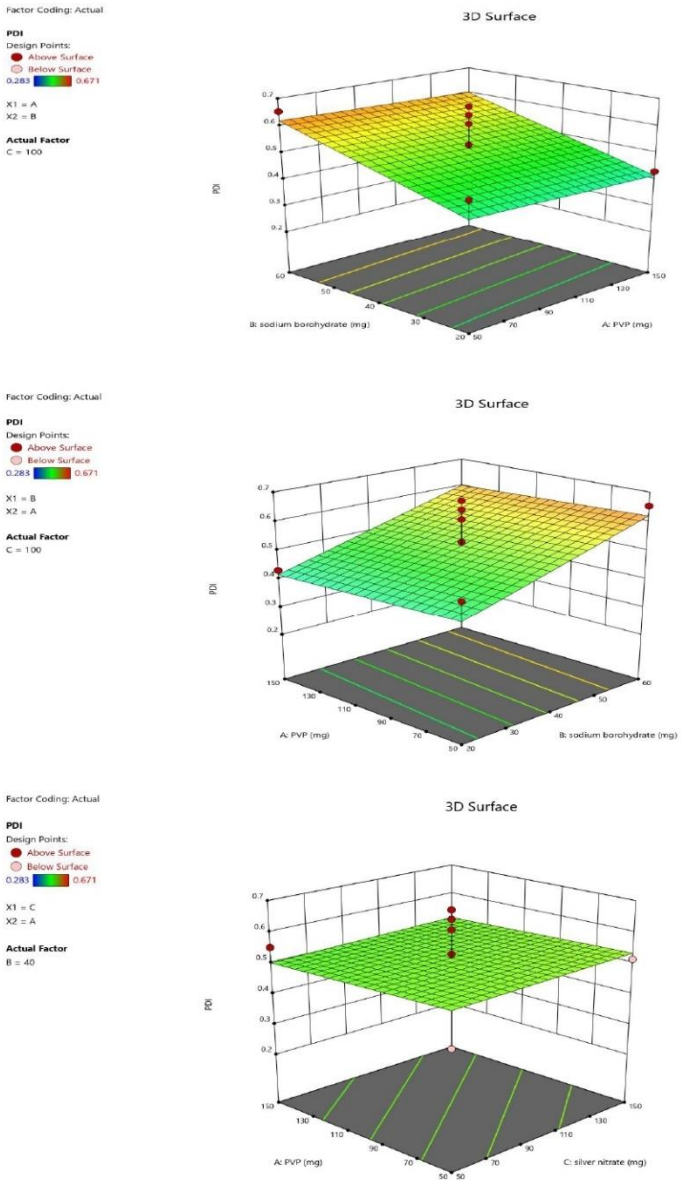

Figure II: Response surface plot (3D) of PDI

FigII,Final coded equation, PDI=0.5088-0.0921A+0.0921B+0. 0064C.Sodium borohydride had a positive influence, while PVP showed negative and silver nitrate had limited effect.

Zeta potential:

Stable ZPs, -13.0mV to – 10.5mV in four runs, shows good colloidal stability.Data demonstrated that factors substantially influence ZP. The polynomial equation is given as:

ZP= -15.00-1.50A+2.75B – 1.20C+0.80AB – 1.10AC – 0.90BC+0.65A^2 – 0.55B^2+0.45C^2.

PVP negatively influences ZP, whereas Sodium borohydride influences positively. Silver nitrate shows a mild negative effect. Quadratic model was recommended because of higher adjusted R^2(0.7374). Negative predicted R^2 (-0.5582) shows low performance. Linear and 2FI models were unsatisfactory owing to lack of fit and low predictive ability. Quadratic model was substantial (F=5.99, P=0.0138), efficiently defining variations in ZP. Significant factors ($p<0.05$) comprised A, B, C, B^2 and C^2.(AB,AC, BC)and A^2 were not considerable ($p>0.1$),simplification of model. The lack of fit (F=6.57, P=0.0503) was slightly satisfactory, showing need of refinement. Model exhibited R2=0.8851, Adjusted R2=0.7374 and Adequate Precision = 7.157, showed a evident signal to noise ratio. Final coded equation,

ZP=19.94-2.14A-1.87B-2.53C+1.74AB-1.87AC-2.36BC+1.45A^2+2.72B^2+3.11C2.

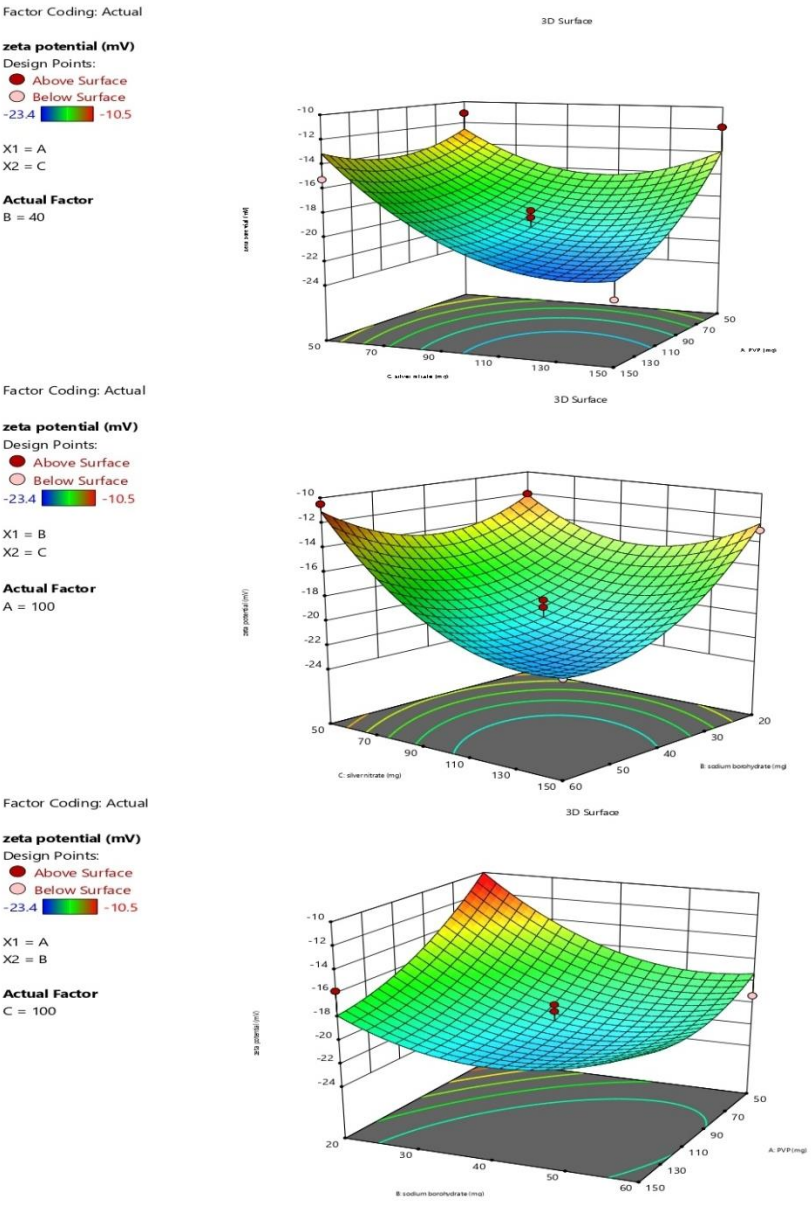

Figure III: Response surface plot (3D) of ZP

Fig III, this forecasts zeta potential depending factor levels, including coefficients showing comparative impact. Optimised formulation was with 76.411nm particle size,0.427PDI and -17.590mV ZP, with a desirability of 0.576, thereby ensuring stability, uniformity and effective drug delivery. ANOVA analysis of particle size, PDI and ZP were given in tables IV,V and VI respectively, and optimization solution in table VII.

Table IV: ANOVA analysis for Particle Size

Source	Sum of Squares	Df	Mean Square	F-value	P -value	
Model	34439.20	9	3826.58	65.57	< 0.0001	significant
A-PVP	6923.70	1	6923.70	118.64	< 0.0001	
B-sodium borohydrate	903.34	1	903.34	15.48	0.0056	
C-silver nitrate	4337.53	1	4337.53	74.33	< 0.0001	
AB	340.03	1	340.03	5.83	0.0465	
AC	3119.78	1	3119.78	53.46	0.0002	
BC	97.32	1	97.32	1.67	0.2376	
A^2	5076.14	1	5076.14	86.98	< 0.0001	
B^2	7780.38	1	7780.38	133.32	< 0.0001	
C^2	3941.02	1	3941.02	67.53	< 0.0001	
Residual	408.51	7	58.36			
Lack of Fit	326.55	3	108.85	5.31	0.0702	not significant
Pure Error	81.96	4	20.49			
Cor Total	34847.71	16				

Table V: ANOVA analysis for PDI

Source	Sum of Squares	Df	Mean Square	F-value	p-value	
Model	0.0689	3	0.0230	3.48	0.0473	significant
A-PVP	0.0007	1	0.0007	0.1038	0.7525	
B-sodium borohydrate	0.0679	1	0.0679	10.29	0.0069	
C-silver nitrate	0.0003	1	0.0003	0.0493	0.8278	
Residual	0.0858	13	0.0066			
Lack of Fit	0.0582	9	0.0065	0.9399	0.5719	not significant
Pure Error	0.0275	4	0.0069			
Cor Total	286.28	16				

Table VI: ANOVA analysis for ZP

Source	Sum of Squares	Df	Mean Square	F-value	p-value	
Model	253.39	9	28.15	5.99	0.0138	significant
A-PVP	36.68	1	36.68	7.81	0.0268	
B-sodium borohydrate	27.90	1	27.90	5.94	0.0450	
C-silver nitrate	51.36	1	51.36	10.93	0.0130	
AB	12.11	1	12.11	2.58	0.1524	
AC	13.95	1	13.95	2.97	0.1285	
BC	22.28	1	22.28	4.74	0.0659	
A^2	8.81	1	8.81	1.87	0.2133	
B^2	31.12	1	31.12	6.62	0.0368	
C^2	40.76	1	40.76	8.67	0.0216	
Residual	32.89	7	4.70			
Lack of Fit	27.34	3	9.11	6.57	0.0503	not significant
Pure Error	5.55	4	1.39			
Cor Total	286.28	16				

Table VII: Optimized solution.

Number	PVP	sodium borohydrate	silver nitrate	particle size	PDI	zeta potential	Desirability
1	119.972	22.683	115.901	76.411	0.427	-17.590	0.576

Scanning Electron Microscopy (SEM):

SEM analysis revealed nanoparticle aggregation into larger clusters with a rough, porous surface, indicating smaller nanoparticles within. This increase surface area, enhancing drug loading and release. Though aggregation could affect dispersion, the surface roughness favours cellular interaction and adhesion.The scale bar (1 µm) shows nanoparticles < 100 nm, an ideal size for drug delivery, promoting cellular uptake and bioavailability. This morphology supports drug absorption and controlled release.

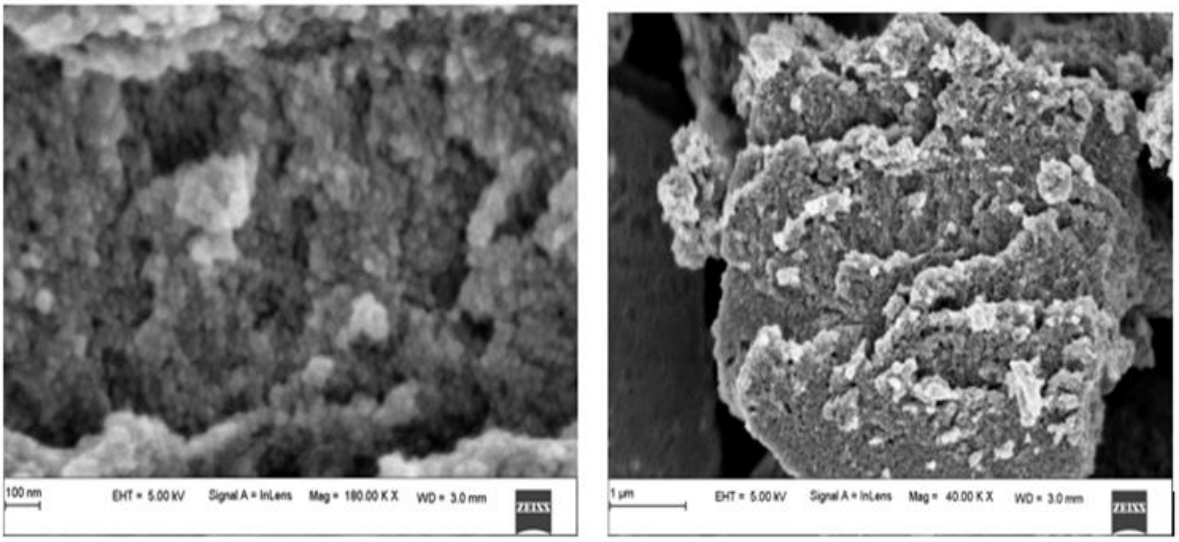

Fig IV: SEM (100X & 40X)

Transmission electron microscopy(TEM):

TEM affirmed the nanoparticles spherical shape (70 - 80 nm), uniformly dispersed with minimal agglomeration, indicating good colloidal stability. Controlled agglomeration could benefit sustained drug release, enhancing cellular uptake, bioavailability, and therapeutic efficacy. The selected area electron diffraction pattern displayed distinct rings, establishing the crystalline nature of the silver nanoparticles. Observed lattice spacing confirms the face-cantered cubic structure, supporting formulation stability.

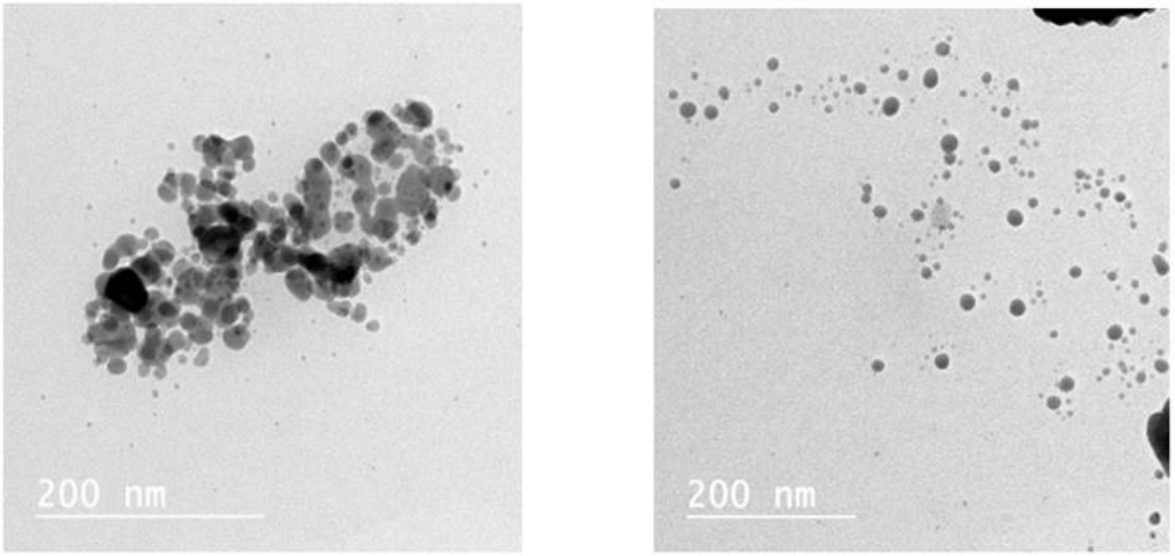

Fig V:TEM

Fourier Transform Infrared Spectroscopy (FT-IR) Analysis:

FTIR revealed presence of functional groups from both Roflumilast and nanoparticles. Peaks at 1652.7 cm^{-1} (C=O stretching), 1000 cm^{-1} (C–F stretching),1557.24 cm^{-1} (amide group), and 1596 cm^{-1} (C=C aromatic stretching) shows successful incorporation of Roflumilast. Peak at 3091 cm^{-1} (C–H stretching) and 3854.04 cm^{-1} (O–H stretching) indicates silver nanoparticle formation.

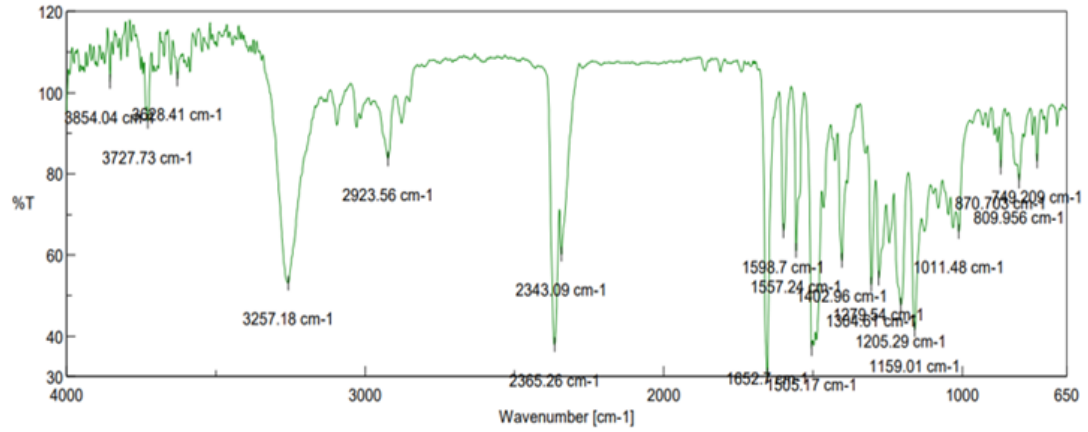

Roflumilast

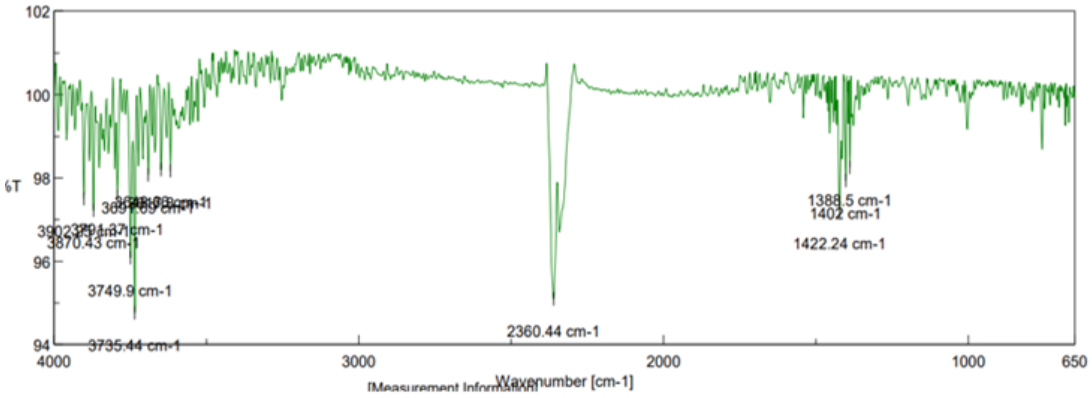

Roflumilast loaded Silver Nanoparticles

Figure VI represents the FTIR analysis.

***In-Vitro* Release Study:**

Fig VII presents cumulative release of Roflumilast from R-AgNPs over 24 hours. The initial release of 15.2±1.4% within 0.5 hours suggests rapid therapeutic effect, succeeding 21.7±1.9% at 1 hour and 34.5±3.1% at 2 hours indicating sustained release effect. By 8 hours, the release reached 65.3±3.9%, and was 92.7±4.4% after 24 hours, confirming prolonged therapeutic efficacy. Higuchi's model (R^2=0.9913) affirms a diffusion- controlled mechanism, assuring extended therapeutic efficacy, decreased dose frequency and better patient compliance.

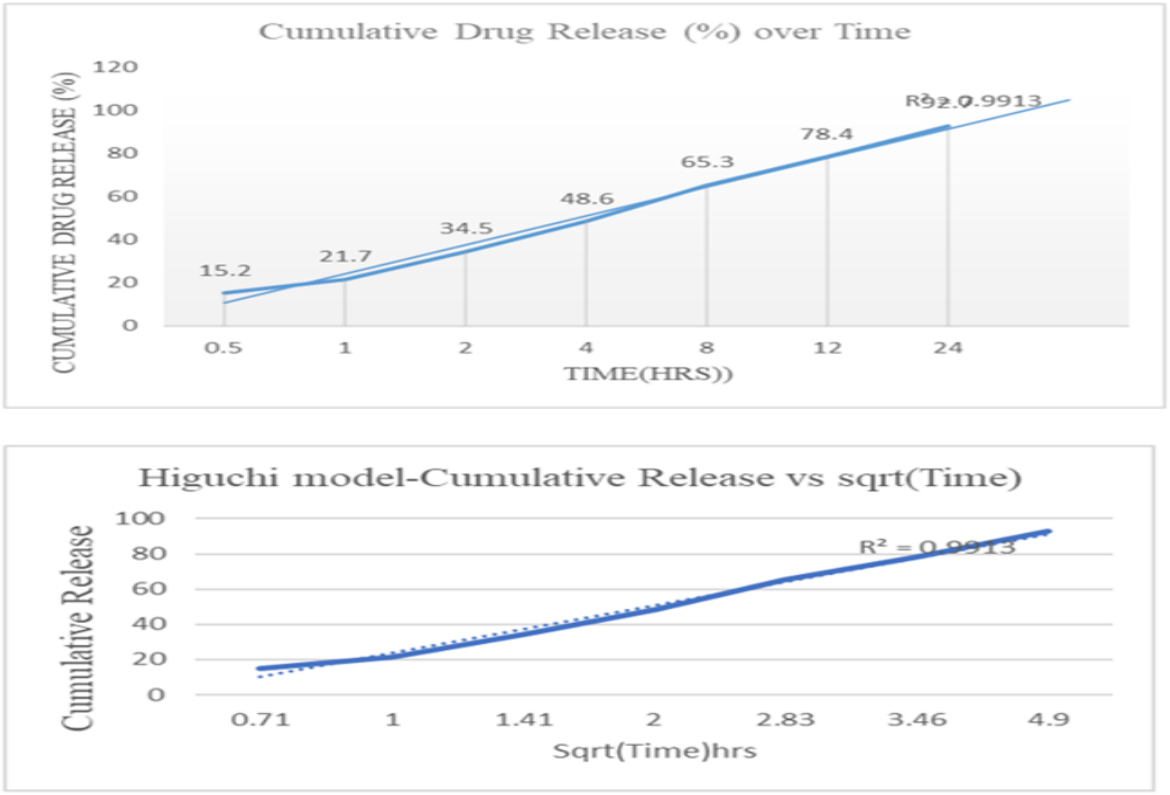

Fig VII: Drug release profile

4. DISCUSSION

BBD optimized influence of PVP, sodium borohydride, and silver nitrate on particle size, PDI, and ZP. Stability and drug deliver efficiency was affirmed from small particle size, low PDI, and high ZP. Sodium borohydride positively influences particle size, impacting nucleation rate and growth. Whereas, silver nitrate had negative effect due to controlled ion availability restricting agglomeration. Their interaction showed reduced particle size. PVP and sodium borohydride increased PDI, causing polydispersity. Meanwhile, silver nitrate reduced PDI, ensuring uniformity. Model was appropriate, even though by low predicted R^2. Sodium borohydride increased ZP while PVP and silver nitrate reduced stability. Quadratic model, having higher adjusted R^2, revealed excellent colloidal stability. Thus, optimization helped to attain stable formulation with effective drug delivery system.

FTIR confirmed Roflumilast's stability in nanoparticles. Broad peaks of O-H/N-H stretching indicates hydrogen bonding. C-H stretching was less distinct, possibly by interaction with encapsulation material. While C=O stretching was less defined, amide II/N-H bending remained evident. C=C stretching indicated amide group. Shifts in fingerprint region, implied physical adsorption. C-F stretching shows fluorine group after encapsulation. Minor spectral shifts may contribute to enhanced drug stability and bioavailability.

SEM analysed improved surface area for drug release from nanoparticle aggregation. Porous clusters and surface roughness improves cellular interaction and adhesion. Particle size formed (<100nm) was optimal for controlled release and bioavailability. TEM analysed spherical nanoparticles with controlled aggregation that aided colloidal stability, sustained drug release and enhanced bioavailability.

Drug release revealed an initial burst release, securing prompt therapeutic effect, succeeded by sustained release over 24 hours. This biphasic pattern complies with diffusion-controlled kinetics (Higuchi-model), while also revealing zero order release aspects, assuring constant release profile over time.

5. CONCLUSION

The study highlights successful incorporation of Roflumilast into silver nanoparticles, optimizing particle size, PDI, and ZP using Box Behnken Design. Lower silver nitrate concentrations produced smaller nanoparticles, while higher sodium borohydride concentrations led to larger particle size. PVP and sodium borohydride influenced PDI, with higher concentrations resulting in less uniformity. Analysis of ZP revealed that higher sodium borohydride concentrations enhanced stability, while PVP slightly reduced it. A promising optimized stability and uniformity was brought about by fine tuning the

reagents' concentration. Drug release follows diffusion-controlled kinetics (Higuchi model) with zero-order characteristics. The current research helps boost the bioavailability and therapeutic efficacy of Roflumilast-loaded silver nanoparticles in dermal inflammatory diseases. Extending the study into modification of nanocarriers pave way for targeted therapeutic outcomes which promises next generation dermatological treatments.

Abbreviations: PDE4: Phosphodiesterase 4; USA: United States of America;UV:Ultraviolet; KBR:Potassium bromide; PBS:phosphate-buffered saline; ANOVA : Analysis of Variance

REFERENCES

[1] Chandraker SK, Kumar R. Biogenic biocompatible silver nanoparticles: a promising antibacterial agent. Biotechnology and Genetic Engineering Reviews. 2024 Nov 1;40(4):3113-47.

[2] Ivanova N, Gugleva V, Dobreva M, Pehlivanov I, Stefanov S, Andonova V. Silver Nanoparticles as Multi-Functional Drug Delivery. InNanomedicines 2018. IntechOpen.

[3] Bieber T. Disease modification in inflammatory skin disorders: opportunities and challenges. Nature Reviews Drug Discovery. 2023 Aug;22(8):662-80.

[4] Drakos A, Vender R, Torres T. Topical roflumilast for the treatment of psoriasis. Expert Review of Clinical Immunology. 2023 Sep 2;19(9):1053-62.

[5] Routray SB, Patra CN, Raju R, Panigrahi KC, Jena GK. Lyophilized SLN of Cinnacalcet HCl: BBD enabled optimization, characterization and pharmacokinetic study. Drug Development and Industrial Pharmacy. 2020 Jul 2;46(7):1080-91.

[6] Rampado R, Peer D. Design of experiments in the optimization of nanoparticle-based drug delivery systems. Journal of controlled release. 2023 Jun 1;358:398-419.

[7] Rai P, Pandey A, Pandey A. Optimization of sugar release from banana peel powder waste (BPPW) using box-behnken design (BBD): BPPW to biohydrogen conversion. International Journal of Hydrogen Energy. 2019 Oct 4;44(47):25505-13.

[8] Kamarudin D, Hashim NA, Ong BH, Che Hassan CR, Abdul Manaf N. Synthesis of silver nanoparticles stabilised by pvp for polymeric membrane application: a comparative study. Materials Technology. 2022 Apr 16;37(5):289-301.

[9] Kesharwani P, Md S, Alhakamy NA, Hosny KM, Haque A. QbD enabled azacitidine loaded liposomal nanoformulation and its in vitro evaluation. Polymers. 2021 Jan 13;13(2):250.

[10] Veljković VB, Veličković AV, Avramović JM, Stamenković OS. Modeling of biodiesel production: Performance comparison of Box–Behnken, face central composite and full factorial design. Chinese Journal of Chemical Engineering. 2019 Jul 1;27(7):1690-8.

[11] Hossain MS, Jahan S, Rahman SA, Rahman M, Kumar D, Paul S, Rajbangshi JC. Design expert software assisted development and evaluation of empagliflozin and sitagliptin combination tablet with improved in-vivo anti-diabetic activities. Heliyon. 2023 Mar 1;9(3).

[12] Quintero-Quiroz C, Acevedo N, Zapata-Giraldo J, Botero LE, Quintero J, Zárate-Triviño D, Saldarriaga J, Pérez VZ. Optimization of silver nanoparticle synthesis by chemical reduction and evaluation of its antimicrobial and toxic activity. Biomaterials research. 2019 Dec 19;23(1):27.

[13] Dawadi S, Katuwal S, Gupta A, Lamichhane U, Thapa R, Jaisi S, Lamichhane G, Bhattarai DP, Parajuli N. Current research on silver nanoparticles: synthesis, characterization, and applications. Journal of nanomaterials. 2021;2021(1):6687290.

[14] Karmakar SA. Particle size distribution and zeta potential based on dynamic light scattering: Techniques to characterize stability and surface charge distribution of charged colloids. Recent Trends Mater. Phys. Chem. 2019;28:117-59.

[15] Savchenko E, Velichko E. New techniques for measuring zeta-potential of colloidal system. InSaratov Fall Meeting 2018: Optical and Nano-Technologies for Biology and Medicine 2019 Jun 3 (Vol. 11065, pp. 432-438). SPIE.

[16] Craparo EF, Cabibbo M, Scialabba C, Giammona G, Cavallaro G. Inhalable formulation based on lipid–polymer hybrid nanoparticles for the macrophage targeted delivery of Roflumilast. Biomacromolecules. 2022 Jul 28;23(8):3439-51.

[17] Varia U, Joshi D, Jadeja M, Katariya H, Detholia K, Soni V. Development and evaluation of ultradeformable vesicles loaded transdermal film of boswellic acid. Future Journal of Pharmaceutical Sciences. 2022 Sep 8;8(1):39.

[18] Tkachenko Y, Niedzielski P. FTIR as a method for qualitative assessment of solid samples in geochemical research: a review. Molecules. 2022 Dec 13;27(24):8846.

[19] Bhuyar P, Rahim MH, Sundararaju S, Ramaraj R, Maniam GP, Govindan N. Synthesis of silver nanoparticles using marine macroalgae Padina sp. and its antibacterial activity towards pathogenic bacteria. Beni-Suef University Journal of Basic and Applied Sciences. 2020 Dec;9:1-5.

[20] Yang S. Characterization of silver nanoparticles. Polymer Nanocomposites Based on Silver Nanoparticles: Synthesis, Characterization and Applications. 2021:83-107.

[21] Pramanik S, Mohanto S, Manne R, Rajendran RR, Deepak A, Edapully SJ, Patil T, Katari O. Nanoparticle-based drug delivery system: the magic bullet for the treatment of chronic pulmonary diseases. Molecular Pharmaceutics. 2021 Sep 7;18(10):3671-718.